 doi:10.20944/preprints202005.0098.v1

Expression and characterization of a novel recombinant cytotoxin II from *Naja naja oxiana* venom: A potential treatment for breast cancer

Afshin Derakhshani[1#], Nicola Silvestris[2,3#], Khalil HajiAsgharzadeh[1], Sara Mahmoudzadeh[4,5], Mohammad Fereidouni[6], Angelo Virgilio Paradiso[7], Oronzo Brunetti[2], Deyhim Atarod[8], Hossein Safarpour[6], Behzad Baradaran[1,9*]

1- Immunology Research Center, Tabriz University of Medical Sciences, Tabriz, Iran.
2- Medical Oncology Unit - IRCCS Istituto Tumori "Giovanni Paolo II" of Bari, Italy.
3- Department of Biomedical Sciences and Human Oncology DIMO—University of Bari, Italy.
4- Student Research Committee, Birjand University of Medical Sciences, Birjand, Iran.
5- Department of Immunology, Faculty of Medicine, Birjand University of Medical Sciences, Birjand, Iran
6- Cellular & Molecular Research center, Birjand University of Medical Sciences, Birjand, Iran.
7- Experimental Oncology and Biobank Management Unit - IRCCS Istituto Tumori "Giovanni Paolo II", Bari, Italy.
8- Institute of Biochemistry and Biophysics (I.B.B.), University of Tehran, Tehran, Iran.
9- Department of Immunology, Faculty of Medicine, Tabriz University of Medical Sciences, Tabriz, Iran.

# The first two authors contributed equally to this work.

Behzad Baradaran, Immunology Research Center, Tabriz University of Medical Sciences, Tabriz, Iran. Tel: +98 413 3371440; Fax: +98 413 3371311. Email: baradaranb@tbzmed.ac.ir

Hossein Safarpour, Cellular and Molecular Research Center, Birjand University of Medical Sciences, Birjand, Iran. Tel: +98-5632381258; Email: H.safarpour@bums.ac.ir

Preprints (www.preprints.org) | NOT PEER-REVIEWED | Posted: 6 May 2020 doi:10.20944/preprints202005.0098.v1

Abstract

Breast cancer (BC) is among the leading causes of mortality from cancer in women. Many of the available anticancer drugs have various side effects. Therefore, researchers are seeking novel anticancer agents particularly from natural compounds and in this regard, snake venom is still one of the main sources of drug discovery. Previous studies showed potential anticancer effects of Cytotoxin II (CTII) from *Naja naja oxiana* against the different types of cancers. In this study, a pET-SUMO-CTII vector was transformed into SHuffle® T7 Express, an *Escherichia coli* strain, for recombinant protein expression (rCTII) and the cytotoxic effects of this protein was assessed in MCF-7 cells. The flow cytometry assay was applied to measure the apoptosis and cell cycle. Also, mRNA levels of the Bax, Bcl2, P53, caspase-3, caspase-8, caspase-9, caspase-10, matrix metalloproteinases (MMP)-3, and MMP-9 were analyzed by quantitative real-time PCR to determine the underlying cellular pathways affected by rCTII. The results of this study showed that treatment with 4 µg mL^{-1} of rCTII enhanced apoptosis through the intrinsic and extrinsic pathways. Also, the increase of the cells' proportion in the sub-G1 phase as well as a reduction in S phase was observed. In addition, the expression of MMP-3 and MMP-9 was decreased in the treated group in comparison to the control group that may contribute to the reduced migratory ability of tumor cells. These experimental results indicate that rCTII has anti-proliferative potential, and so this protein could be a potential drug for BC therapy in combination with other drugs.

Keywords: Breast Cancer; Snake Venom; Cytotoxin II, Recombinant protein, Apoptosis; Cell Cycle Progression; Cytotoxicity

Preprints (www.preprints.org) | NOT PEER-REVIEWED | Posted: 6 May 2020 doi:10.20944/preprints202005.0098.v1

Graphical Abstract

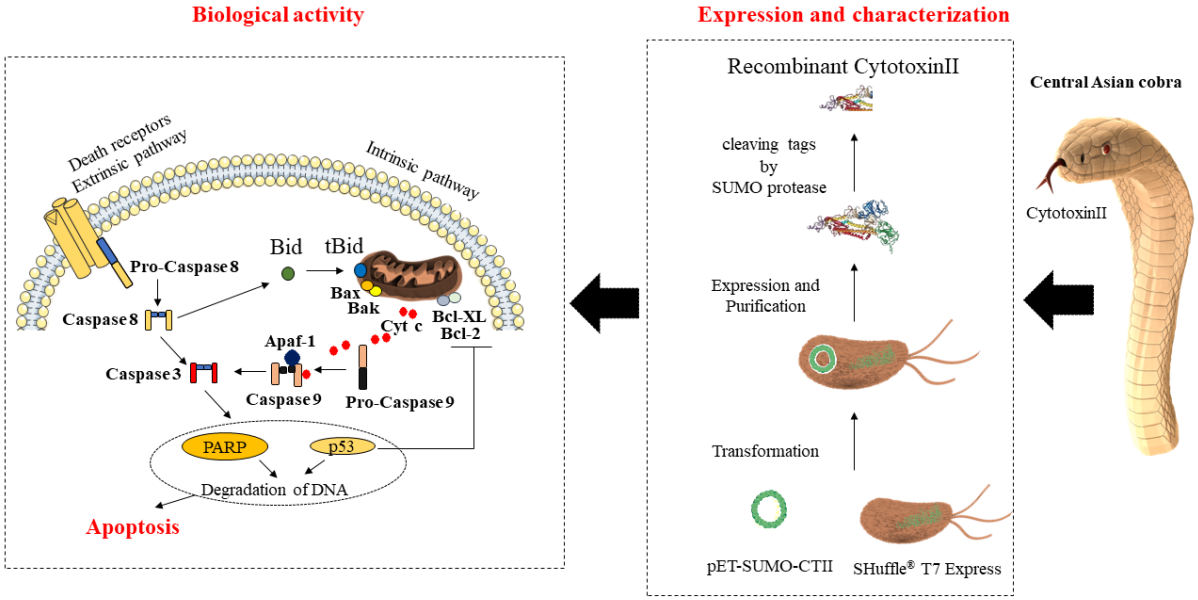

The expressed recombinant Oxus cobra CTII in SHuffle® T7 Express can induce apoptosis through the intrinsic and extrinsic pathways in the Breast Cancer cell line.

Preprints (www.preprints.org) | NOT PEER-REVIEWED | Posted: 6 May 2020 doi:10.20944/preprints202005.0098.v1

1. Introduction

Breast cancer (BC) is the most frequent type of malignancy in women and is also the main cause of cancer mortality in females [1]. Globally, it is reported that more than one million people are diagnosed with BC every year with about 400,000 women death annually, accounting for 14 percent of the total cancer deaths [2, 3]. The conventional treatment methods for BC, like other cancers, include surgery, chemotherapy, and radiotherapy [4]. The main purpose of these treatments is to exterminate tumors while enhancing the survival rate of the patients. On the other hand, the emergence of therapy resistance is an important obstacle to achieving this purpose [5]. Considering the harmful side-effects presented in the classical cancer therapeutics, the search for novel active drugs for different malignancies is one of the fundamental aims of the biotechnological research and pharmaceutical industries [6]. During the last twenty years, BC therapeutic drugs have been mainly identified in the field of immunotherapy. Regardless of the significant efficacy of monoclonal antibodies e.g. trastuzumab, BC treatment strategies remain unsatisfactory [7, 8]. Hence, several advanced, safer, and more efficient biotherapeutics have been developed in laboratories for treating tumors. During recent years, bispecific antibodies [9], oncolytic viruses [10], antibody-drug conjugates (ADCs) [11], and toxins [12] have gradually become research hotspots. In the case of toxins, several compounds from snakes or other venomous animals have largely studied and shown promising anti-cancer properties [13-16]. Snake venoms consist of various components including protein, peptide, and other bioactive mixtures, which are isolated from the snakes ' venom glands and injected by unique fangs of snakes to debilitate and digest their prey. Despite its toxicity, a variety of isolated proteins and peptides from snake venoms are functional as pharmaceutical agents with different properties [17, 18].

Recent studies have shown that a group of 60-70 amino acids polypeptides, generally named cytotoxins, which can kill cancer cells [19-21]. Two specific cytotoxins have identified as cytotoxin-I (CTI) and cytotoxin-II (CTII) from *Naja naja oxiana* have been identified for their cytotoxic and cell membrane disturbing actions [22]. Although both cytotoxins have about 80% homology in amino acid sequences, their cytotoxic properties are different [23]. In 2014, Ebrahim *et al.* investigated the potential anticancer of CTII (4 μg mL^{-1}) in the MCF-7 cell line. They indicated that CTII has potent anti-BC impacts in the MCF-7 cells via intrinsic apoptosis pathways [24]. More recently, Attarde *et al.* purified NN-32, a very similar toxin to CTII from Naja naja venom with significant cytotoxicity in both MCF-7 and MDA-MB-231 cell lines in a dose- and time-dependent fashion [25]. In spite of all promising data about the

Preprints (www.preprints.org) | NOT PEER-REVIEWED | Posted: 6 May 2020 doi:10.20944/preprints202005.0098.v1

anti-cancer effects of CTII, more researches need to identify the structure and molecular mechanisms of its action. Considering the limited availability of natural sources and large quantities that are needed for researches, the production of the recombinant form of CTII could provide enough CTII and promote the investigations. Herein, in this research, we expressed recombinant Oxus cobra CTII in SHuffle® T7 Express, an *Escherichia coli* (*E. coli*), and characterized the secondary structure. Finally, the biological activity of the recombinant CTII (rCTII) protein, as well as anti-proliferative mechanisms have been investigated in BC cell line.

2. Materials and methods

2.1. Bacterial strain and cell culture

E. coli SHuffle® T7 Express was used as the expression host for the production of the requested protein. The MCF-7 cell line was obtained from the National Cell Bank of Iran. The cells were cultured in RPMI-1640 medium, which supplied with 10% fetal bovine serum (FBS) and penicillin/streptomycin mixtures (Gibco, Carlsbad, CA, USA) and were grown at 37 °C incubator in a humidified atmosphere with 5% CO_2 level. Each experiment has been repeated three times.

2.2. Construction of pET-SUMO-CTII

The DNA sequence corresponding to the mature form of CTII peptide (Naja oxiana, UniProtKB: P01441) was codon-optimized for *E. coli* cell expression. This sequence was synthesized with ubiquitin-like modifier (SUMO) tag by Bioneer Inc. (Daejeon, South Korea) and cloned into pET-28a (+) vector (Invitrogen, California, United States) containing an N-terminal polyhistidine tag. Figure 1 illustrates the mechanisms and strategies for synthesizing the fusion gene.

2.3. Expression of SUMO-fusion proteins in E. coli

The constructed pET-SUMO-CTII vector was transformed into SHuffle® T7 Express for protein expression. An individual colony of transformed bacteria was transferred into 10 mL of Luria Bertani (LB) broth medium (Merk, Germany) and spent overnight at 37 °C in a shaking incubator. Next, 1 mL of this medium was mixed with 100 mL of sterilized LB medium and 50 µg mL^{-1} Kanamycin. Following that, this medium kept at 37 °C and 150 rpm

Preprints (www.preprints.org) | NOT PEER-REVIEWED | Posted: 6 May 2020 doi:10.20944/preprints202005.0098.v1

till they reached the exponential phase ($OD_{600\ nm}$ of 0.4-0.6), then the expression processes continued through the addition of 1 mM Isopropyl-β-D-thiogalactopyranoside (IPTG) and kept for 4 h at 28 °C. At the end of expression time, the pellets of induced bacteria were gathered after 20 min 7000 g centrifuge at 4 °C and analyzed by 12% gel SDS-PAGE.

2.4. Purification of SUMO-fused protein

The bacterial pellets were resuspended in lysis buffer, and then the suspension was sonicated five-six times on ice at 60-70% pulse for 20 s with 30 s pauses intervals in between to maintain a low temperature. Then, bacterial debris was separated after 30 min 7000 g centrifuge at 4 °C. The final fusion protein was added to the affinity chromatography column packed with immobilized metal ion-affinity chromatography (IMAC) (Qiagen, Germany) as we performed in the previous study [26]. The eluted proteins were examined on SDS-PAGE and collected for further tests.

2.5. Quantification of protein

Determining the size and purity of the obtained protein was analyzed by reducing SDS-PAGE and subsequent staining with silver nitrate. The concentration of the protein was evaluated by both UV-Vis spectroscopy at 280 nm and the Bradford method using standard BSA protein (Sigma Aldrich, Germany).

2.6. Western and dot immunoblotting analysis

For western blotting, purified rCTII and BSA were applied to SDS-PAGE. Then, the proteins were transferred to the nitrocellulose membrane (NC) (Sigma Aldrich, Germany). After blocking with skimmed milk 2% (w/v) in PBS, the membrane was incubated with an anti-His-tag monoclonal antibody (Biolegend, USA) diluted in 0.5% (v/v) Tween 20 in PBS buffer. Then after several times washing with PBST buffer (20 mM Tris and 150 mM NaCl, pH 7.6, 0.1% Tween-20), the blots were treated with goat anti-mouse IgG (GAM-HRP) as a secondary antibody (Biolegend, USA) (diluted 1:3000) and ECL kit (Roche Diagnostics GmbH) was applied to signal detection. For dot blot analysis, 10 µL of purified rCTII, BSA (negative control), and anti-His-tag antibody (positive control) were blotted on NC membrane at 1 cm intervals and left to dry for 1 h at room temperature (RT). Unreacted sites on the membrane were blocked by immersing the membranes by 2% skimmed milk and incubated for 1 h at RT and washed three times with PBST. NC membranes were incubated with GAM-HRP as a secondary antibody (Biolegend, USA) (diluted 1:3000) for 1 h at RT followed by

Preprints (www.preprints.org) | NOT PEER-REVIEWED | Posted: 6 May 2020 doi:10.20944/preprints202005.0098.v1

washing three times with TBST. The target proteins were detected and visualized by BCIP and NBT (Sigma, Deisenhofen, Germany).

2.7. Cleavage of SUMO fusions

After 1 mg mL^{-1} dilution of the eluted target protein and addition of 10 units of SUMO protease, the mixture was kept for 1 h at 4 °C in a high salt buffer (50 mM Tris-HCl, pH 8.0, 0.15 M NaCl, 1 mM DTT). After incubation time, the proteins were transferred to a Ni-NTA resin column (Qiagen, Hilden, Germany) to take the rCTII. The SUMO, uncleaved-SUMO-CTII, and SUMO protease became bound to the Ni-NTA column and just the rCTII was eluted after washing with elution buffer. Imidazole was removed by dialysis with 1x PBS buffer (5.85 g L^{-1} NaCl, 4.72 g L^{-1} Na_2HPO_4, 2.64 g L^{-1} $NaH_2PO_4.2H_2O$, pH = 7.2) for overnight at 4 °C. The final target proteins were checked on SDS-PAGE and the samples were saved at -80 °C for subsequent structural characterization with CD spectroscopy and identification of its biological activities through different molecular biology techniques.

2.8. rCTII secondary structure analysis by CD spectroscopy

To determine the secondary structure of rCTII of SHuffle® T7 Express, a far-UV CD experiment was performed using a model 410 circular dichroism spectrometer (Aviv Biomedical Inc., Lakewood, NJ) in a standard quartz cuvette with 1 mm thickness at 20 °C. Further detailed conditions of CD spectroscopy were identical to those described by Hoffmann and colleagues [27]. For this analysis, 400 µg mL^{-1} of recombinant protein in 1x PBS buffer pH 7.0 was used. Spectra were adjusted for buffer additions and transformed to mean residue ellipticity according to the previous study [28]. The changes in secondary structure content were calculated with CDNN 2.1 software.

2.9. Apoptosis assay

2.9.1. Annexin V/PI assay

MCF-7 cells were seeded in 6-well plates at a density of 3×10^5 cells and examined in control and treated groups. After 24 h treatment with 4 µg mL^{-1} of rCTII, Annexin-V/PI assay was used. In brief, the cells were washed two times with PBS and then treated with 100 µL of Annexin V/PI containing binding buffer. Then, the cells were kept in the dark for 15 min and after that, quickly assessed by the flow cytometry (FCM) instrument (Miltenyi Biotech, GmbH, Germany).

Preprints (www.preprints.org) | NOT PEER-REVIEWED | Posted: 6 May 2020 doi:10.20944/preprints202005.0098.v1

2.9.2. Cell cycle analysis

For investigating the cell cycle arrest properties of rCTII, the MCF-7 cells were pelleted 24 h after 4 µg mL^{-1} incubation. Following that, these cells were fixed with 50 % ethanol, treated with 5 mg mL^{-1} RNase A (Daejeon, Korea), and then used 50 µg mL^{-1} of PI solution for staining, and assessed by FCM system for cell cycle progression study.

2.10. Wound healing assay

The migration rate of the MCF-7 cells was assessed by using a wound-healing assay. For this analysis, approximately 3×10^5 of MCF-7 cells were cultured in the six-well plates for 24 h, and in confluency of around 90%, the wound was created by the use of the yellow pipette tip across the cell monolayer to make an open gap to mimicking the wound. Then the cell debris washed away with a serum-free medium. Wells were divided into two groups (a treated group with 4 µg mL^{-1} of rCTII and the untreated groups). The cells were photographed under the inverted microscope and kept for the next 24 h at the incubator and permitted to migrate to the wound zone and images of the plate were collected at 0, 12, and 24 h. The migratory ability of the cells was analyzed by determining the distances between the edges of the wound.

2.11. RNA preparation, cDNA synthesis, and qRT-PCR

The expression of apoptosis and migratory genes (Bax, Bcl2, P53, caspase-3, caspase-8, caspase-9, caspase-10, MMP-3, and MMP-9) was analyzed by qRT-PCR. For this examination, in each experimental group, cells were subjected to RNA extraction using TRIzol reagent (RiboEx). After cDNA synthesis using a kit (Biofact, South Korea), the qRT-PCR was performed utilizing light cycler 96 (Roche Diagnostics, Mannheim, Germany). The data were analyzed using $2^{-\Delta\Delta CT}$ method. The sequences of each primer are shown in *table 1*.

2.12. Statistical Analysis

All data were presented as mean ± standard deviation (SD). Statistical significance of differences between variables was assessed via T-test analyses by using GraphPad Prism 6 software (San Diego, CA, USA). The *P*-value below 0.05 was deemed relevant.

3. Results

3.1. Expression and purification of His-SUMO-CTII fusion protein

Preprints (www.preprints.org) | NOT PEER-REVIEWED | Posted: 6 May 2020 doi:10.20944/preprints202005.0098.v1

To prevent intracellular aggregation of the rCTII, the protein was expressed under the T7 promoter with a small SUMO tag. SUMO was used to help in the proper folding of the protein and therefore in the production of soluble proteins. In addition, a SUMO specific protease was used to the elimination of the SUMO tag and production of N-terminal amino acids free proteins [29]. SHuffle® T7 Express cells were first successfully transformed with pET-28a vector containing His-SUMO-CTII sequence and then induced for expression of interest protein by 1 mM of IPTG at 28 °C. The induction analysis of SDS-PAG proved the generation of recombinant major-band protein at approximately 18.5 kDa that was compatible with the anticipated molecular weight (MW) of His-SUMO-CTII (Figure 2). SUMO-CTII fusion protein with N-terminal His-tag was purified by affinity chromatography on Ni-NTA column. SUMO-CTII was eluted from the column and analyzed by SDS-PAGE which appeared with an Mw of ~18.5 kDa (Figure 2).

3.2. Immunoblot analysis

The identity of purified His-SUMO-CTII was confirmed by dot and western blot analysis. For dot blot analysis, the purified His-SUMO-CTII and Anti-His Tag (positive control) were detected while BSA as negative control didn't detect (Figure 3A). Also, for western blot analysis, as shown in figure 3B, His-SUMO-CTII was detected while the BSA as negative control didn't detect.

3.3. Proteolytic digestion and scale-up purification of rCTII

Purified SUMO-CTII was subjected to cleavage reaction by SUMO protease for removal of the SUMO tag. The presence of two bands of rCTII and SUMO on 12% SDS-PAGE gel confirmed the successful cleavage of the SUMO tag (Figure 2). These results verified that the tertiary structure of SUMO was properly formed in *E. coli* and identified by SUMO protease. rCTII was purified from cleavage reaction by Ni-NTA column and then collected in the flow through. After removal of the SUMO tag, purified rCTII was resolved by 12% SDS-PAGE that showed a single band of ~6.6 kDa (Figure 2). The data from Bradford assay has also exhibited that the concentration of rCTII was 400 µg mL^{-1} in *E. coli* SHuffle® T7 Express.

3.4. Biophysical analysis of rCTII

The CD approach aims to the rapid investigation of the secondary structure and environmentally caused structural alterations of proteins [30]. In this study, the secondary structure of rCTII was studied by CD at 25 °C and the obtained spectrum was analyzed with

Preprints (www.preprints.org) | NOT PEER-REVIEWED | Posted: 6 May 2020 doi:10.20944/preprints202005.0098.v1

CDNN software (version 2.1) according to previous studies and shown in figure 4 [31]. The content of different secondary structures of rCTII was measured and the results included 6.106 % α-helix, 35.87 % antiparallel β-sheet, 5.15 % parallel β-sheet, 18.7 % β-turn, and 34.16 % random coil. These findings revealed that the β-sheet and random coils are the dominant secondary structures of rCTII.

3.5. CTII enhanced apoptosis of MCF-7 cells

3.5.1. CTII induced the early and late apoptosis of MCF-7 cells

To evaluate the potential anti-proliferative function of rCTII, we assessed the effects of this recombinant protein on apoptosis of MCF-7 cells through Annexin-V/PI staining. The CTII treated and untreated cells incubated for 24 h. In Annexin-V/PI assay, Annexin V positive (+) and PI-negative (−) cells were characterized as early apoptotic cells and double-positive Annexin V (+) and PI (+) cells were considered as late apoptotic cells. In treated MCF-7 cells after 24 h exposure with rCTII, the percentage of Annexin V+/PI+ (late apoptosis) and Annexin V+/PI− (early apoptosis) cells were statistically significant than untreated control cells (Figure 5A and 5B). The summarized apoptotic data was demonstrated in figure 5C. In addition to this flow cytometry study, the apoptosis-related genes were assessed by Real-time PCR to further validation of the effect of rCTII on apoptosis.

3.5.2. CTII induced the arrest of the cells in the sub-G1 phase

Cell cycle analysis of the cells that incubated with 4 μg mL^{-1} of rCTII presented in figure 6. The results showed that there is an increasing ratio of the cells in the sub-G1 group (apoptotic cells) after treatment. The proportion of the cells in the sub-G1 phase was 0% in the control group in comparison with 35.5% in treated cells. In addition, a decreasing trend in the S phase in treated cells compared to the control group was observed in the study (Figure 6).

3.6. CTII treatment reduced the cells migration ability of MCF-7 cells

A wound-healing approach was done to assess the migration rate of MCF-7 cell line in rCTII treated and untreated groups. The wound space was recorded at 0, 12, and 24 h. The results indicated that the migration of MCF-7 cells was significantly inhibited after 12 h and 24 h treatment with rCTII (Figure 7). Moreover, for further evaluation of the migration rate of MCF-7 cells following rCTII treatment the MMP-3 and MMP-9 genes expression were evaluated to find the effect of rCTII on the migration of the cells.

Preprints (www.preprints.org) | NOT PEER-REVIEWED | Posted: 6 May 2020 doi:10.20944/preprints202005.0098.v1

3.7. CTII treatment induced the apoptosis and reduced the migration-related mRNA expression levels of MCF-7 cells

To evaluate the underlying pathways of apoptosis, the expression of P53, Bcl2, Bax, caspase-3, caspase-8, caspase-9, and caspase-10 was evaluated by real-time PCR in the control and rCTII treated group. Our result illustrated that this protein potentially activated both intrinsic and extrinsic pathways related to apoptosis. P53, Bax, caspase-3, caspase-8, caspase-9, caspase-10 (p-value:0.0002, p-value<0.0001, p-value<0.0001, p-value <0.0001, p-value:0.002, and p-value<0.0001 respectively) were upregulated in the treated group in comparison with control, on the other hand, Bcl2 (p-value<0.0001) as an anti-apoptotic factor was down-regulated in the treated group. Furthermore, the expression of MMP-3 and MMP-9 (p-value<0.0001and p-value<0.0001 respectively) was assessed and showed significant down-regulation in the treated group compared with control which may indicate a reduction of migration ability of the cells in this cancer cell line. The results have shown in figure 8.

4. Discussion

BC is the most frequent cause of cancer death in women [24]. Like the other cancers, there are some options for BC cancer therapy. Several compounds of venomous species have generally shown anti-cancer pharmacological properties [32]. Researchers indicated cytotoxic effects of snake venom can diminish and damage tumor cells. Kim *et al.* showed the L-amino acid oxidase which was isolated from the venom of the king cobra, *Ophiophagus hannah* can inhibit cell proliferation in fibroblastic sarcoma, ovarian cancer, colorectal cancer, stomach cancer, and murine melanoma cell lines according to [3H] thymidine uptake approach [33]. The function of this enzyme can be linked to thymidine incorporation blockade and DNA interaction [33]. Zhang *et al.* extracted ACTX-6 protein, which has 98 kDa Mw that could enhance the Hela cells' apoptosis [34]. The isolated cardiotoxic-cytotoxic protein with 6.76 kDa Mw from the monocled cobra (*Naja kaouthia*) significantly, could inhibit human leukemic U937 and K562 cells growth in a dose- and time-dependent fashion [35]. In another research, NN-32 which was a purified venom from Indian *Naja naja* through ion-exchange chromatography displayed cytotoxic effects on Ehrlich ascites carcinoma (EAC) mice, which decreased the tumor size and enhanced the survival of animals [36]. The Caspian cobra (*Naja naja oxiana*), also known as the Central Asian cobra or Oxus cobra, is a highly venomous cobra species found in Central Asia within the Elapidae family. *Naja naja oxiana* venom has an anticancer role in many different types of cell lines [37-39]. Researchers showed that the

Preprints (www.preprints.org) | NOT PEER-REVIEWED | Posted: 6 May 2020 doi:10.20944/preprints202005.0098.v1

IC_{50} values of Caspian cobra venom were 26.59, 21.17, and 47.1 µg mL^{-1} for the cell lines HepG2, DU145, and MDCK respectively [37]. The idea of this research was obtained from Ebrahim *et al.* researches which investigated the potential anticancer of native CTII (4 µg mL^{-1}) in the MCF-7 cell line [40]. By using recombinant methods, we can easily express heterologous genes in pro and/or eukaryotic hosts, i.e. genes that they normally do not express. In this regard, the *E. coli* is one of the important hosts of recombinant protein production due to its rapid growth, simple handling, and cost-effectiveness [26]. In the present study, for the first time, we successfully transformed the pET-SUMO-CTII vector into SHuffle® T7 Express and effectively expressed rCTII in this bacterium as shown in figure 2. We purified and then cleaved the rCTII and considered by using SDS-PAGE and immune blotting assays (Figure 3). As sown in figure 2 the Mw of the current protein was 6.6 kDa similar. There was no study related to the production of rCTII in the bacteria as well as PDB or secondary structure analysis of rCTII. Many different techniques are introduced for the analysis of protein structures, such as Attenuated Total Reflection (ATR) Fourier Transform Infrared (FTIR) spectroscopy. This spectroscopy method is a great potential analytical approach to promote protein crystallization and investigations of the effect of surface protein behaviors [41]. Moreover, CD spectroscopy is an incredibly powerful tool for fast determination of the secondary structure, folding, and binding features of the proteins [42]. For the characterization of this protein, after the production of rCTII by SHuffle® T7 Express, we used CD spectroscopy for the characterization of this novel protein. The content of different secondary structures of rCTII was determined via CDNN software (Figure 4), and it contains 6.106 % α-helix, 35.87 % antiparallel β-sheet, 5.15 % parallel β-sheet, 18.7 % β-turn, and 34.16 % random coil. This experiment was the first study to exhibit the effects of rCTII from SHuffle® T7 Express against breast carcinoma cells. Multiple physiological and biological processes involved in the appropriate cell development processes and homeostasis-pathogenesis and many diseases associated with the impaired apoptosis process. Apoptosis has an important impact on maintaining the balance among cell death and division and avoiding apoptosis contributes to excessive cell proliferation leading to various diseases, including many types of cancers. Due to minimal inflammation that occurs during apoptosis of the cells, the establishment of anticancer drugs to improve apoptosis has received more interest in cancer research [43]. In the present research, we applied different techniques for the detection of molecular pathways, which involved in apoptosis in MCF-7 cell line after treatment with 4 µg mL^{-1} of rCTII. We chose this concentration based on previous research on the natural type of CTII in MCF-7 cells [40]. Annexin V/PI staining indicated a significant

Preprints (www.preprints.org) | NOT PEER-REVIEWED | Posted: 6 May 2020 doi:10.20944/preprints202005.0098.v1

translocation of phosphatidylserine (PS) from the inside of cancer cells to the outside after exposure to rCTII. The rCTII increased the early apoptosis in the treated cells in comparison with control cells. In addition, the increasing rate in the late apoptosis ratio has been shown in the treated cells in comparison with controls (figure 5). The cell cycle progression analysis showed a reduction of S phase and increasing proportions of cells in the sub-G1 group (apoptotic cells). Our results confirmed the previous study which showed that ~88 percent of the cells treated with rCTII were in the sub-G1 phase [44]. In this study, our recombinant CTII showed more effectiveness in comparison to the isolated extract from the venom source in the 4 µg mL^{-1} concentration. As indicated by many researchers, CII has potent anti-cancer effects in the MCF-7 cell line, which are induced via the intrinsic apoptosis pathways [24]. More recently, Attarde *et al.* purified NN-32, a very similar toxin to CTII amino acid sequences from *Naja naja* venom with cytotoxicity versus MCF-7 and MDA-MB-231 cells and the IC_{50} values were 2.5 and 6.7 µg mL^{-1} respectively [25]. Yang *et al.* which isolated Cardiotoxin-3 (CTX-3), from *Naja naja atra* venom, showed the induced apoptosis of K562 cells occurred through up-regulating Bax and endonuclease G and downregulating of Bcl-X [45]. The other study also confirmed LAAO isolated from Agkistrodon acutus snake venom arrests cancer cells during the sub-G1 phase of the cell cycle and induces apoptosis via the Fas signaling cascade in A549 cells [25]. The process of apoptosis through the mitochondrial pathway induces loss of mitochondrial membrane potential (MMP), the release of cytochrome c, and activation of caspases genes. Our study showed the expression of P53, Bax, caspase-3, caspase-8, caspase-9, and caspase-10 significantly upregulated after treatment with rCTII. Although we showed the down-regulation of Bcl2 in the treated group in compression with the controls. These findings illustrate the capability of rCTII to activate the intrinsic and extrinsic pathways of apoptosis simultaneously. The previous study confirmed our finding that showed CTII extracted from native form up-regulated the caspase-9 in MCF-7 cells after treatment and their observations confirmed the possibility that apoptosis was mediated by the intrinsic pathway [24]. The other research on NKCT1 toxin from *Naja Koauthia* venom showed that after conjugation with gold nanoparticles, it shows anticancer effects in EAC cells. GNP-NKCT1 induced caspase-dependent apoptosis in EAC cells, induced a late apoptotic stage, and arrested the cells in the G0/G1 phase [46].

Metastasis is a multi-step mechanism that contains the movement and invasion of cancer cells and defines as a signature for malignancy. The next step in our study was the assessment of the potential effects of rCTII on the migration of MCF-7 cells. Migration was evaluated by

Preprints (www.preprints.org) | NOT PEER-REVIEWED | Posted: 6 May 2020 doi:10.20944/preprints202005.0098.v1

wound healing assay, which is the complex, dynamic movement of the cells. Observation of the motility of living cells is an important tool for calculating the rate of movement to the area produced by the initial cut. The ideal condition is when the wound gap filled slowly by the cells over a prolonged time, which ensures that the investigated agent prevents the movement of cancer cells. Figure 7 indicates the effects of rCTII on the wound healing assay. In untreated cells, the migration was very dynamic after only 12 and 24 h, but the wound's closure was completed after 24 h. By using a 4 μg mL^{-1} of rCTII, the motility of the MCF-7 cells was inhibited in 12 and 24 h. Furthermore, it is well understood that MMPs are essential to the process of cancer cell movement [24, 37]. Therefore, after the scratch test, we investigated to understand if our rCTII had similar effects on MMP-3 and MMP-9 expression. The findings indicate that this protein down-regulated the expression of MMP-3 and MMP-9 in the breast cancer cell line at the mRNA level and confirmed our scratch test results.

5. Conclusion

In this novel *in vitro* study, the recombinant form of CTII successfully produced and it's bioactivity against MCF-7 cell line confirmed by different methods. The results of this study indicate that rCTII has anti-proliferative effects and can be considered as a promising candidate for breast cancer therapy. More studies particularly on animal models or through clinical trials are needed to prove our findings.

Conflict of interest

The authors declare that there is no conflict of interest.

Author Contributions:

Afshin Derakhshani the first author of the manuscript, design the project, perform the experiments, and write the initial version of the manuscript. Nicola Silvestris, Khalil HajiAsgharzadeh, Sara Mahmoudzadeh, and Deyhim Atarod participate in analyzing the data and completing the work. Mohammad Fereidouni, Angelo Virgilio Paradiso, and Oronzo Brunetti read the manuscript and contributing in the English editing of the manuscript, and also helping in data categorization. Behzad Baradaran and Hossein Safarpour: the corresponding authors of the manuscript, financially support the work and supervise the project and also contributing to the revising of the main text of the manuscript.

 doi:10.20944/preprints202005.0098.v1

Conflicts of Interest: The authors declare that the research was conducted in the absence of any commercial or financial relationships that could be construed as a potential conflict of interest.

 doi:10.20944/preprints202005.0098.v1

References

1. Li, T., et al., *Descriptive epidemiology of breast cancer in China: incidence, mortality, survival and prevalence.* 2016. **159**(3): p. 395-406.
2. Parkin, D.M. and L.M.J.T.b.j. Fernández, *Use of statistics to assess the global burden of breast cancer.* 2006. **12**: p. S70-S80.
3. Anderson, B.O., et al., *Breast cancer in limited-resource countries: health care systems and public policy.* 2006. **12**: p. S54-S69.
4. Waks, A.G. and E.P.J.J. Winer, *Breast cancer treatment: a review.* 2019. **321**(3): p. 288-300.
5. Liyanage, P.Y., et al., *Nanoparticle-mediated targeted drug delivery for breast cancer treatment.* 2019.
6. Falzone, L., S. Salomone, and M. Libra, *Evolution of Cancer Pharmacological Treatments at the Turn of the Third Millennium.* Front Pharmacol, 2018. **9**: p. 1300.
7. Esteva, F.J., et al., *Immunotherapy and targeted therapy combinations in metastatic breast cancer.* 2019. **20**(3): p. e175-e186.
8. Derakhshani, A., et al., *Overcoming trastuzumab resistance in HER2-positive breast cancer using combination therapy.* Journal of Cellular Physiology, 2020. **235**(4): p. 3142-3156.
9. Rader, C.J.C.O.i.B., *Bispecific antibodies in cancer immunotherapy.* 2020. **65**: p. 9-16.
10. Russell, L., et al., *Oncolytic viruses: priming time for cancer immunotherapy.* 2019: p. 1-17.
11. Yaghoubi, S., et al., *Potential drugs used in the antibody–drug conjugate (ADC) architecture for cancer therapy.* 2020. **235**(1): p. 31-64.
12. Li, L., J. Huang, and Y.J.T. Lin, *Snake venoms in cancer therapy: past, present and future.* 2018. **10**(9): p. 346.
13. Lewis, R.J. and M.L.J.N.r.d.d. Garcia, *Therapeutic potential of venom peptides.* 2003. **2**(10): p. 790-802.
14. Fernandes-Pedrosa, M.F., et al., *Toxins from venomous animals: gene cloning, protein expression and biotechnological applications.* 2013: p. 23-71.
15. Chatterjee, B.J.C.t.i.m.c., *Animal Venoms have Potential to Treat Cancer.* 2018. **18**(30): p. 2555-2566.
16. de Souza, J.M., et al., *Animal toxins as therapeutic tools to treat neurodegenerative diseases.* 2018. **9**: p. 145.
17. Calderon, L.A., et al., *Antitumoral activity of snake venom proteins: new trends in cancer therapy.* 2014. **2014**.
18. Jridi, I., et al., *The small subunit of Hemilipin2, a new heterodimeric phospholipase A2 from Hemiscorpius lepturus scorpion venom, mediates the antiangiogenic effect of the whole protein.* Toxicon, 2017. **126**: p. 38-46.
19. Sinaei, N., et al., *Potential Anticancer Activity of Caspian Cobra Venom Through Induction of Oxidative Stress in Glioblastoma Cell Line.* 2019. **89**(4): p. 1161-1166.
20. Fakhri, A., et al., *Naja naja oxiana venom fraction selectively induces ROS-mediated apoptosis in human colorectal tumor cells by directly targeting mitochondria.* 2017. **18**(8): p. 2201.
21. Attarde, S.S., S.V.J.B.C. Pandit, and A. Medicine, *Cytotoxic activity of NN-32 toxin from Indian spectacled cobra venom on human breast cancer cell lines.* 2017. **17**(1): p. 503.
22. Aripov, T., et al., *Central Asian cobra venom cytotoxins-induced aggregation, permeability and fusion of liposomes.* 1989. **8**(5): p. 459-473.

23. Gasanov, S.E., et al., *Naja naja oxiana Cobra Venom Cytotoxins CTI and CTII Disrupt Mitochondrial Membrane Integrity: Implications for Basic Three-Fingered Cytotoxins.* PLOS ONE, 2015. **10**(6): p. e0129248.
24. Ebrahim, K., et al., *Anticancer activity of cobra venom polypeptide, cytotoxin-II, against human breast adenocarcinoma cell line (MCF-7) via the induction of apoptosis.* 2014. **17**(4): p. 314-322.
25. Attarde, S. and S. Pandit, *Cytotoxic activity of NN-32 toxin from Indian spectacled cobra venom on human breast cancer cell line.* Clinical Therapeutics, 2017. **39**(8): p. e72-e73.
26. Derakhshani, A., et al., *Optimization of induction parameters, structure quality assessment by ATR-FTIR and in silico characterization of expressed recombinant polcalcin in three different strains of Escherichia coli.* Int J Biol Macromol, 2019. **138**: p. 97-105.
27. Hoffmann, A., et al., *Recombinant production of bioactive human TNF-alpha by SUMO-fusion system--high yields from shake-flask culture.* Protein Expr Purif, 2010. **72**(2): p. 238-43.
28. Schmid, F.J.P.s.A.p.a., *Optical spectroscopy to characterize protein conformation and conformational changes.* 1997. **11**.
29. Panavas, T., C. Sanders, and T.R. Butt, *SUMO fusion technology for enhanced protein production in prokaryotic and eukaryotic expression systems*, in *SUMO protocols*. 2009, Springer. p. 303-317.
30. Ding, G.-B., et al., *High-yield expression in Escherichia coli, biophysical characterization, and biological evaluation of plant toxin gelonin.* 2019. **9**(1): p. 19.
31. Ioannou, J., A. Donald, and R.J.F.H. Tromp, *Characterising the secondary structure changes occurring in high density systems of BLG dissolved in aqueous pH 3 buffer.* 2015. **46**: p. 216-225.
32. Rapôso, C., *Scorpion and spider venoms in cancer treatment: state of the art, challenges, and perspectives.* J Clin Transl Res, 2017. **3**(2): p. 233-249.
33. Ahn, M.Y., B.M. Lee, and Y.S. Kim, *Characterization and cytotoxicity of L-amino acid oxidase from the venom of king cobra (Ophiophagus hannah).* Int J Biochem Cell Biol, 1997. **29**(6): p. 911-9.
34. Zhang, L. and L.J. Wei, *ACTX-8, a cytotoxic L-amino acid oxidase isolated from Agkistrodon acutus snake venom, induces apoptosis in Hela cervical cancer cells.* Life Sci, 2007. **80**(13): p. 1189-97.
35. Debnath, A., et al., *A lethal cardiotoxic-cytotoxic protein from the Indian monocellate cobra (Naja kaouthia) venom.* Toxicon, 2010. **56**(4): p. 569-79.
36. Das, T., et al., *Cytotoxic and antioxidant property of a purified fraction (NN-32) of Indian Naja naja venom on Ehrlich ascites carcinoma in BALB/c mice.* Toxicon, 2011. **57**(7): p. 1065-1072.
37. Ebrahim, K., et al., *Anticancer activity a of Caspian cobra (Naja Naja oxiana) snake venom in human cancer cell lines via induction of apoptosis.* Iranian journal of pharmaceutical research: IJPR, 2016. **15**(Suppl): p. 101.
38. Fakhri, A., et al., *Naja naja oxiana venom fraction selectively induces ROS-mediated apoptosis in human colorectal tumor cells by directly targeting mitochondria.* Asian Pacific journal of cancer prevention: APJCP, 2017. **18**(8): p. 2201.
39. Sinaei, N., et al., *Potential Anticancer Activity of Caspian Cobra Venom Through Induction of Oxidative Stress in Glioblastoma Cell Line.* Proceedings of the National Academy of Sciences, India Section B: Biological Sciences, 2019. **89**(4): p. 1161-1166.
40. Ebrahim, K., et al., *Anticancer Activity of Cobra Venom Polypeptide, Cytotoxin-II, against Human Breast Adenocarcinoma Cell Line (MCF-7) via the Induction of Apoptosis.* J Breast Cancer, 2014. **17**(4): p. 314-22.
41. Glassford, S.E., B. Byrne, and S.G. Kazarian, *Recent applications of ATR FTIR spectroscopy and imaging to proteins.* Biochimica et Biophysica Acta (BBA)-Proteins and Proteomics, 2013. **1834**(12): p. 2849-2858.

 doi:10.20944/preprints202005.0098.v1

42. Greenfield, N.J., *Using circular dichroism spectra to estimate protein secondary structure.* Nature protocols, 2006. **1**(6): p. 2876.
43. Jan, R., *Understanding apoptosis and apoptotic pathways targeted cancer therapeutics.* Advanced pharmaceutical bulletin, 2019. **9**(2): p. 205.
44. Ebrahim, K., et al., *Anticancer activity of cobra venom polypeptide, cytotoxin-II, against human breast adenocarcinoma cell line (MCF-7) via the induction of apoptosis.* Journal of breast cancer, 2014. **17**(4): p. 314-322.
45. Yang, S.-H., et al., *Up-regulation of Bax and endonuclease G, and down-modulation of Bcl-X L involved in cardiotoxin III-induced apoptosis in K562 cells.* Experimental & molecular medicine, 2006. **38**(4): p. 435-444.
46. Bhowmik, T., et al., *Influence of gold nanoparticle tagged snake venom protein toxin NKCT1 on Ehrlich ascites carcinoma (EAC) and EAC induced solid tumor bearing male albino mice.* Current drug delivery, 2014. **11**(5): p. 652-664.

Preprints (www.preprints.org) | NOT PEER-REVIEWED | Posted: 6 May 2020 doi:10.20944/preprints202005.0098.v1

Figure legends

Figure 1. Schematic representation of the expression vector pET-SUMO-CTII. rCTII was expressed as a fusion protein with the SUMO.

Figure 2. SDS-PAGE analysis of the purification steps of rCTII. Samples from different purification steps were analyzed by 12% SDS-PAGE. Lane 1: Cell lysate insoluble fraction (centrifugation pellet) of *E. coli* SHuffle® T7 Express pET-SUMO-CTII not induced; Lane 2: Cell lysate insoluble fraction *E. coli* SHuffle® T7 Express pET-SUMO-CTII induced; Lane 3: Pre-stained Protein Ladder (PM2700 Protein Marker, SMOBIO®, Taiwan); Lane 4: purified SUMO-CTII; Lane 5: Purified rCTII after SUMO protease cleavage.

Figure 3. A dot blot (A) and western blotting (B) analysis of His-SUMO-CTII. (A) 1: Ani-His-tag antibody (positive control); 2: Purified His-SUMO-CTII; 3: BSA (negative control). (B) 1: Purified His-SUMO-CTII; 2: BSA.

Figure 4. Circular dichroism (CD) analysis of purified rCTII. The spectrum was recorded with the Aviv CD spectrometer at 20 °C in a 1 mm quartz cuvette. The protein concentration was (400 µg mL^{-1}).

Figure 5. Cell apoptosis was detected by Flow cytometry histograms of cell death assays by the PI method in MCF-7 cells. The cells were treated with CTII and then evaluated for cell cycle distribution at 24 h. Cells were categorized as necrotic (Q1), late apoptotic (Q2), viable (Q3), and early apoptotic cells (Q4). A: untreated group, B: treated group C: early and late apoptotic phase. D: apoptosis induction in two groups. ****$p < 0.0001$ were considered as significant levels compared to the untreated control group.

Figure 6. Flow cytometric analysis of cell death. rCTII decreased the number of cells in the S phase and increased the number of cells in the sub-G1 phase (apoptotic cells). (A) Untreated group. (B) Treated group.

Figure 7. Treated and untreated MCF-7 cells were subjected to scratch wound-healing assays. (A) MCF-7 cells divided into 2 groups including treated and untreated. The wound space was photographed at 0, 12, and 24 h. (B) The number of migrated cells to the wound sides was evaluated and statistically analyzed. Error bars indicate the mean ± SD of independent experiments.

Preprints (www.preprints.org) | NOT PEER-REVIEWED | Posted: 6 May 2020 doi:10.20944/preprints202005.0098.v1

Figure 8. The mRNA expression of candidate genes. The expression of P53, Bcl2, Bax, caspase-3, caspase-8, caspase-9, and caspase-10 was assessed by real-time PCR in the Control and treated group. Our result illustrated this protein potentially activated both intrinsic as well as extrinsic pathways related to apoptosis .Error bars display the ± SD. The independent t-tests assessed the p -values. $p < 0.01$ (**), $p < 0.001$(***), and $p < 0.0001$(****). the (***).

Preprints (www.preprints.org) | NOT PEER-REVIEWED | Posted: 6 May 2020 doi:10.20944/preprints202005.0098.v1

Figure 1.

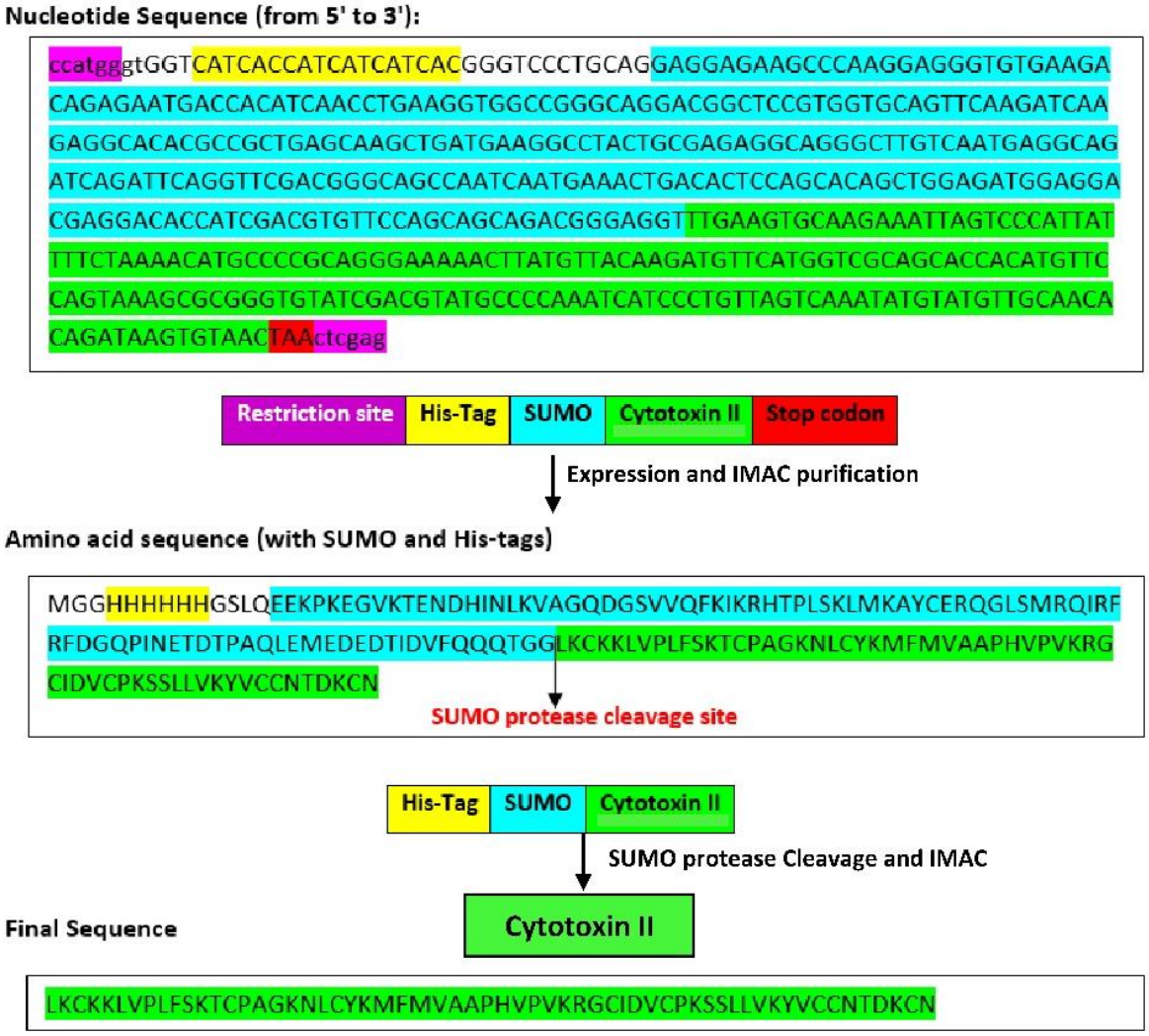

Preprints (www.preprints.org) | NOT PEER-REVIEWED | Posted: 6 May 2020 doi:10.20944/preprints202005.0098.v1

Figure 2.

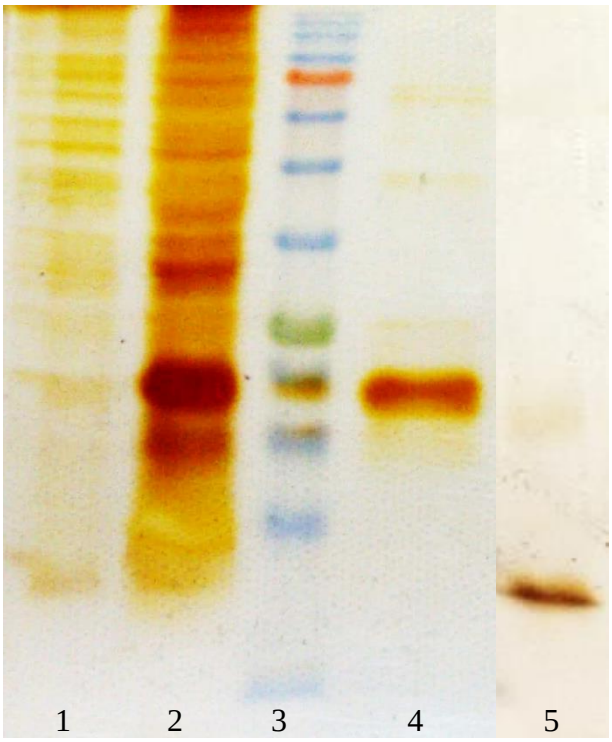

Preprints (www.preprints.org) | NOT PEER-REVIEWED | Posted: 6 May 2020 doi:10.20944/preprints202005.0098.v1

Figure 3.

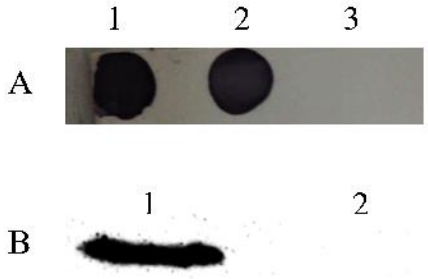

Preprints (www.preprints.org) | NOT PEER-REVIEWED | Posted: 6 May 2020 doi:10.20944/preprints202005.0098.v1

Figure 4.

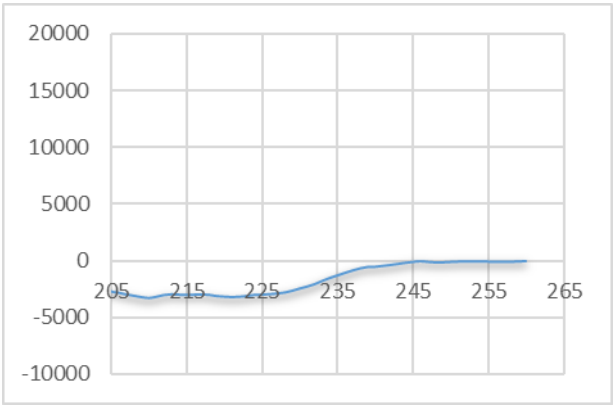

Preprints (www.preprints.org) | NOT PEER-REVIEWED | Posted: 6 May 2020 doi:10.20944/preprints202005.0098.v1

Figure 5.

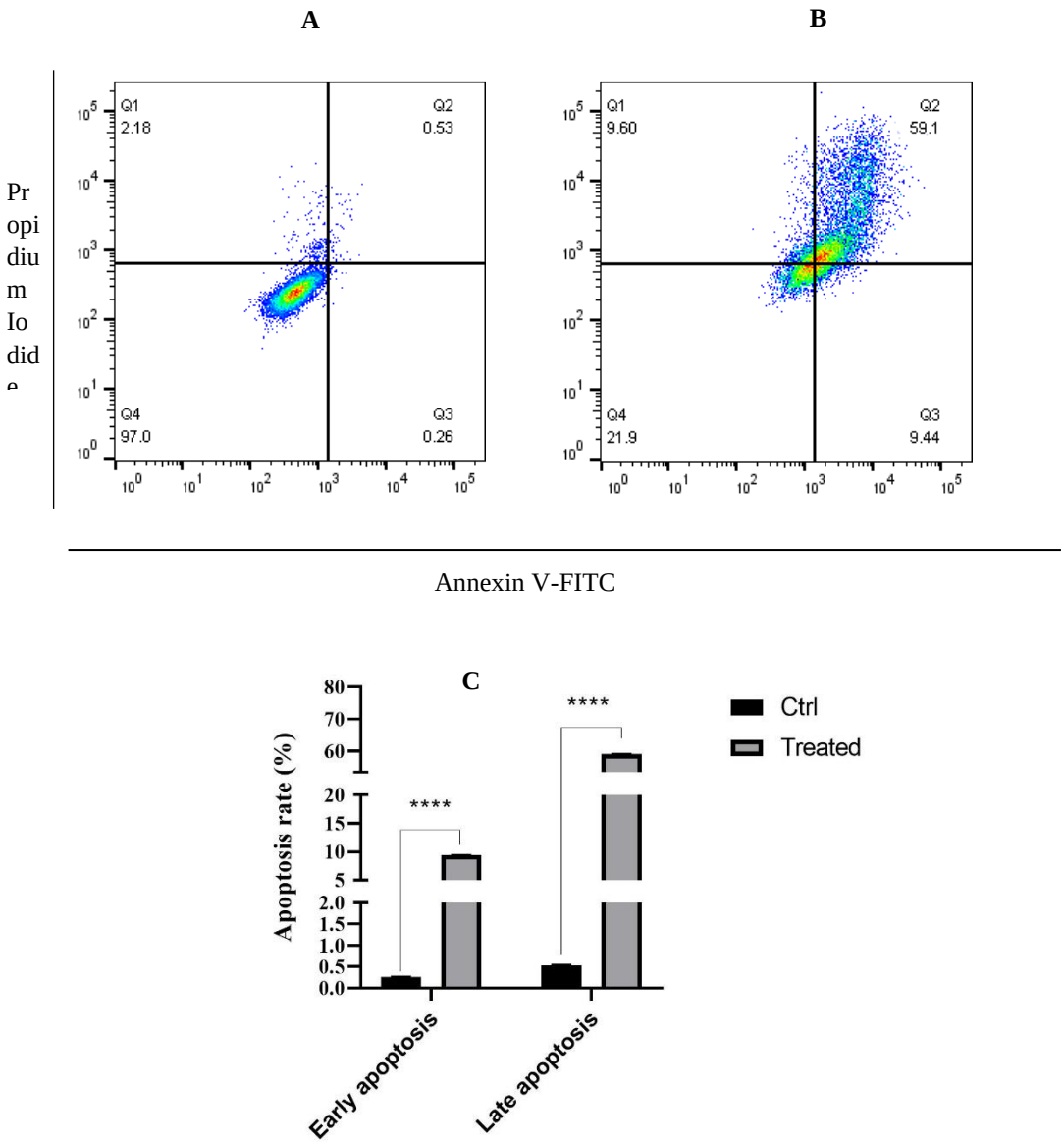

Preprints (www.preprints.org) | NOT PEER-REVIEWED | Posted: 6 May 2020 doi:10.20944/preprints202005.0098.v1

Figure 6.

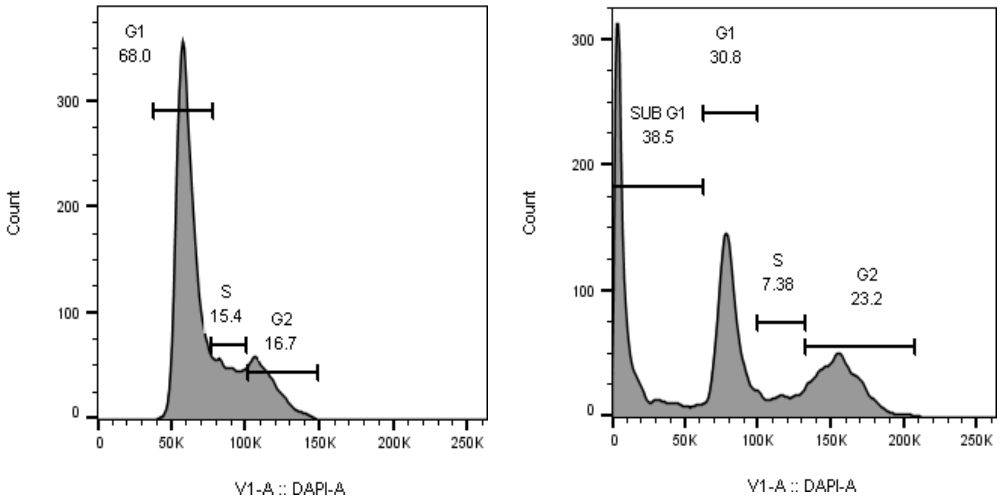

A **B**

Preprints (www.preprints.org) | NOT PEER-REVIEWED | Posted: 6 May 2020 doi:10.20944/preprints202005.0098.v1

Figure 7.

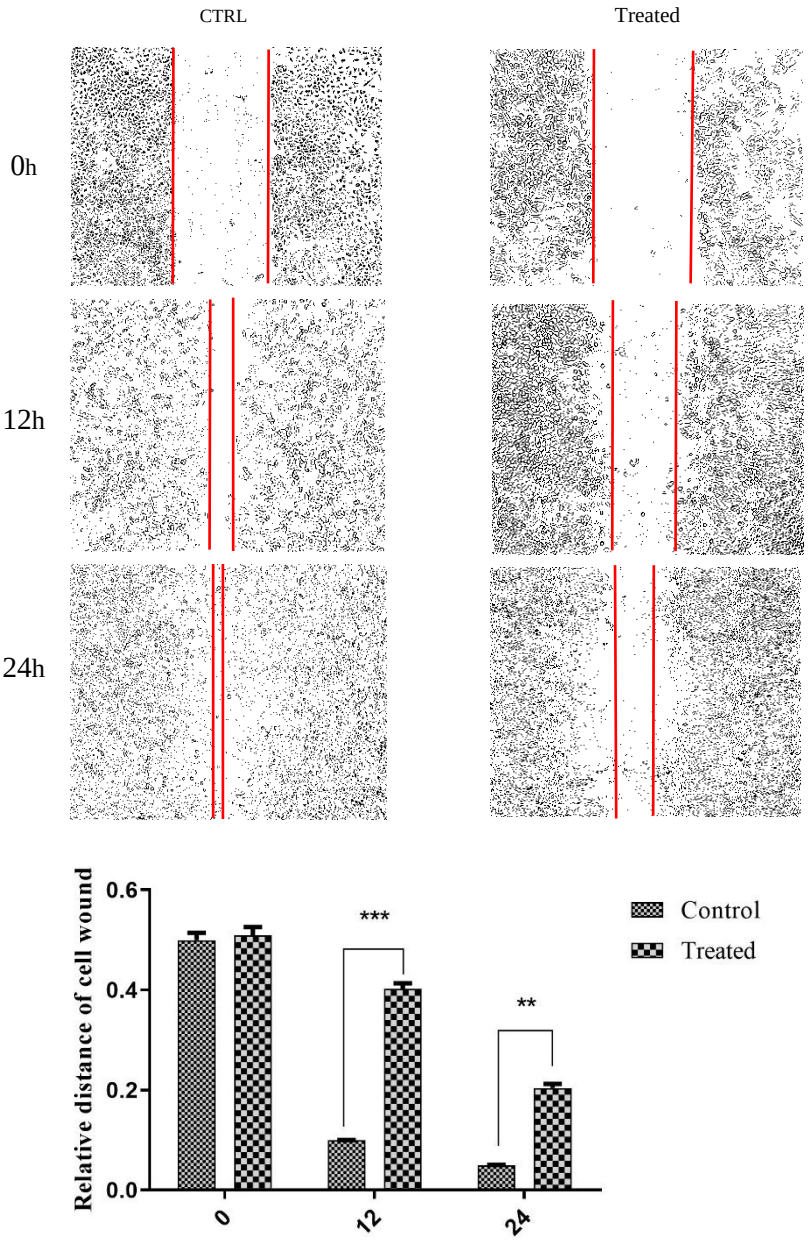

Preprints (www.preprints.org) | NOT PEER-REVIEWED | Posted: 6 May 2020 doi:10.20944/preprints202005.0098.v1

Figure 8.